Acta Crystallographica Section D
Biological Crystallography
ISSN 0907-4449

Thermophilic alcohol dehydrogenase from the mesophile *Entamoeba histolytica*: crystallization and preliminary X-ray characterization

Linda J. W. Shimon,[a]* Moshe Peretz,[b] Edi Goihberg,[b] Yigal Burstein[b] and Felix Frolow[c]

[a]Department of Chemical Services, The Weizmann Institute of Science, Rehovot 76100, Israel, [b]Department of Organic Chemistry, The Weizmann Institute of Science, Rehovot 76100, Israel, and [c]Department of Molecular Microbiology and Biotechnology, Tel Aviv University, Ramat Aviv, Israel

Correspondence e-mail: linda.shimon@weizmann.ac.il

Received 19 September 2001
Accepted 21 January 2002

The tetrameric $NADP^+$-dependent secondary alcohol dehydrogenase from *Entamoeba histolytica* has been crystallized in its apo form. The crystals belong to space group $C222_1$, with unit-cell parameters a = 76.89, b = 234.24, c = 96.24 Å, and diffract to 1.9 Å at liquid-nitrogen temperature. Analysis of the Patterson self-rotation function shows that the crystals contain one dimer per asymmetric unit.

1. Introduction

Increasing our understanding of the stability of enzymes isolated from extremophiles, *i.e.* organisms that function best under extreme conditions of temperatures, ionic strength or pH, has become an important goal in the fields of biochemistry and biotechnology. For this purpose, the alcohol dehydrogenase from mesophilic protozoan parasite *Entamoeba histolytica* (EhADH1; EC 1.1.1.2) has been overexpressed, purified (Goihberg, 2001) and crystallized.

This enzyme belongs to the family of class 1 medium-chain zinc-dependent homotetrameric secondary alcohol dehydrogenases. It is hoped that structural analysis of this protein and its comparison to the previously determined alcohol dehydrogenases from the mesophilic *Clostridium beijerinckii* (CbADH) and the thermophilic *Thermoanaerobium brockii* (TbADH) (Korkhin *et al.*, 1998, 1999) will provide insight into the molecular basis of thermal stability. Sequence and structural comparisons of TbADH and CbADH have shown that differences can be used to pinpoint important features of thermostability. Sequence alignment of EhADH and analysis of thermophilic (TbADH) and mesophilic (CbADH) alcohol dehydrogenase family members has revealed that despite high sequence homologies of 62 and 75%, respectively, there are notable differences in thermostability (Bogin *et al.*, 1998; Peretz *et al.*, 1997). Notwithstanding the high degree of sequence homology in this family of alcohol dehydrogenases, identification of thermostability determinants in such a large molecule is difficult. The addition of a third structure that differs from both the others by approximately 25% dramatically increases the possibility of identifying important interactions and the source of cofactor specificity. Moreover, the thermostability of EhADH falls between that of the thermophilic TbADH and the mesophilic CbADH, making the structural comparison crucial in understanding this system.

2. Materials and methods

2.1. Purification and crystallization

Purified genomic DNA was prepared from a culture of *E. histolytica* and used as a template for the polymerase chain reaction (PCR) with primers based on the EhADH gene (Samuelson *et al.*, 1992). The PCR product was cloned into BS p80 vector (Peretz *et al.*, 1997) and the protein was overexpressed in *Escherichia coli* and purified to homogeneity (Goihberg, 2001). *E. histolytica* alcohol dehydrogenase (EhADH) was crystallized at 293 K by the hanging-drop vapour-diffusion method. Preliminary screening was performed using commercially available kits from Hampton Research. The best of these preliminary conditions, 30% PEG 4K, 100 m*M* Tris pH 8.5 and 200 m*M* sodium acetate (Crystal Screen, condition 22) was taken as a starting point for optimization. Initially, only poorly shaped and twinned tetragonal form crystals could be obtained, which diffracted to a maximum resolution of 3.5 Å; however, extensive screening of pH and the ratio of protein to precipitant in the drop eventually yielded well formed orthorhombic crystals that were chosen for further characterization (Fig. 1). In the final conditions for crystallization, 10 µl of protein stock solution [11.5 mg ml^{-1} protein, 25 m*M* Tris–HCl, 50 m*M* NaCl, 0.1 m*M* DTT (dithiothreitol), 50 m*M* $ZnCl_2$ pH 7.5] was mixed with 1 µl of reservoir solution [14%(*w*/*v*) PEG 8K, 300 m*M* magnesium acetate, 200 m*M* cacodylate buffer pH 6.5]. Initially, precipitate formed; however, after one week crystals appeared and grew to final dimensions of about 0.2 × 0.05 × 0.05 mm over a period of 10 d. For data collection under cryogenic conditions, crystals were transferred to a solution containing 25%(*w*/*v*) ethylene glycol for a period of 10 min before being flash-frozen in

Table 1
Data-collection statistics.

Resolution (Å)	R_{merge}	No. of unique reflections	Completeness (%)	Multiplicity	$\langle I\rangle/\sigma(I)$
20–3.79	0.029	7505	85.2	2.58	27.35
3.78–3.01	0.038	7769	90.9	2.51	24.77
3.01–2.63	0.056	7823	92.0	2.48	15.60
2.63–2.39	0.074	7823	92.6	1.68	12.45
2.39–2.22	0.093	7863	93.1	2.45	9.63
2.22–2.09	0.122	7952	94.4	2.43	7.46
2.09–1.99	0.164	8019	95.4	2.39	5.65
1.99–1.90	0.256	8037	95.9	2.37	3.74
Overall	0.051	62791	92.4	2.46	17.35

liquid nitrogen. Data were collected on beamline ID14-1 at the ESRF (see Table 1 for details).

2.2. X-ray diffraction

A crystal was mounted in a fibre loop and flash-frozen in liquid nitrogen. During measurement, the crystal was kept at 100 K. A full native data set to 1.9 Å resolution was collected as 0.5° oscillation frames, with 30 s per pass and two passes per frame, at a crystal-to-detector distance of 120 mm using a MAR165 CCD detector on beamline ID14-1 at the ESRF with a wavelength of 0.934 Å (Fig. 2). Beam-defining slits were set to 50 × 50 µm. Diffraction data frames were processed with *DENZO* and *SCALEPACK* (Otwinowski & Minor, 1997).

3. Results and discussion

3.1. Results

Diffraction-quality single crystals of EhADH1 were grown by the hanging-drop vapour-diffusion method. The crystals were stable when flash-frozen to 100 K and diffract to at least 1.9 Å at the ESRF synchrotron, with a mosaicity of 0.4°. A full data set to 1.9 Å was collected. Indexing with *DENZO* gave orthorhombic crystals with space group $C222_1$ and unit-cell parameters $a = 76.89$, $b = 234.14$, $c = 96.24$ Å. The relatively long b axis was readily resolved on the detector owing to the use of beam-definition slits set to 50 × 50 µm. Data processing gave an R_{merge} of 5.1% (based on intensities). The data set is 92.4% complete to 1.9 Å (95.9% complete in the range 1.99–1.90 Å) (Table 1). Assuming a calculated molecular weight of 40 150 Da and a dimer per asymmetric unit (see below), the V_M value is 2.77 Å^3 Da^{-1}, which lies in the normal range for globular proteins (Matthews, 1974).

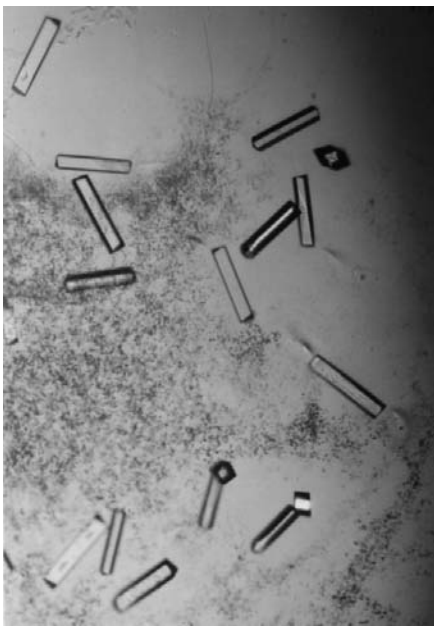

Figure 1
Crystals of *E. histolytica* alcohol dehydrogenase (EhADH). The largest dimension is 0.2 mm.

3.2. Molecular symmetry

The Patterson self-rotation function was calculated with the *POLARRFN* program from the *CCP*4 suite (Collaborative Computational Project, Number 4, 1994). The $\kappa = 180°$ section of the self-rotation stereogram is presented in Fig. 3. Only one non-crystallographic twofold axis ($\varphi = 90$, $\psi = 45°$) can be observed, in agreement with the dimer per asymmetric unit which was inferred from the calculation of the Matthews coefficient. The assumption is then that the biologically active tetramer will be generated by combination of the crystallographic with the non-crystallographic symmetry.

A search for a molecular-replacement solution is in progress using the crystal structures of the homologous enzymes CbADH and TbADH.

We thank the support staff of the ID14-1 beamline at ESRF for their assistance. This research was supported by the Israel Science Foundation (No. 269-00 to YB).

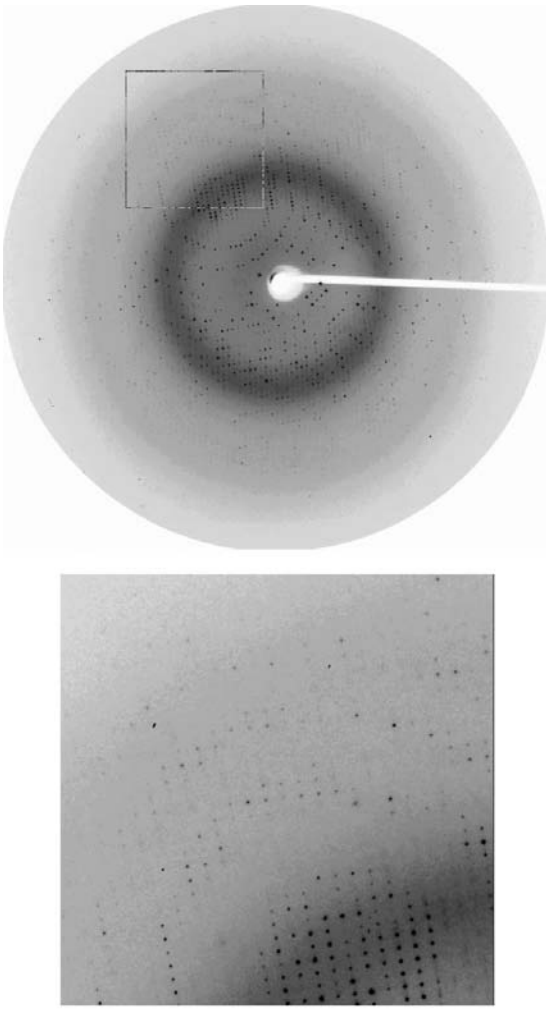

Figure 2
Diffraction pattern of an *E. histolytica* crystal as collected on the ID14-1 experimental station at ESRF. The marked section of the diffraction pattern has been enlarged (below).

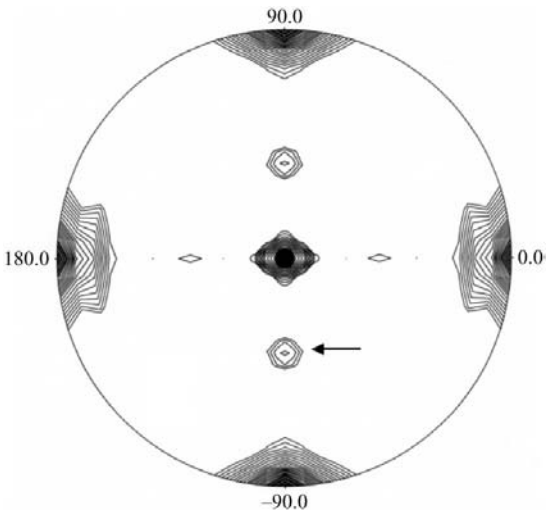

Figure 3
Self-rotation function, section $\kappa = 180°$. Peaks are scaled to the origin peak, which is represented by 100%. Positions of the axes with the related φ angles are marked on the circumference. The twofold axis is marked by an arrow. Contour levels are plotted for all peaks greater than 14% of the origin peak in intervals of 2%.

References

Bogin, O., Peretz, M., Hacham, Y., Korkhin, Y., Frolow, F., Kalb, A. J. & Burstein, Y. (1998). *Protein Sci.* **7**, 1156–1163.

Collaborative Computational Project, Number 4 (1994). *Acta Cryst.* D**50**, 760–763.

Goihberg, E. (2001). MSc thesis. Feinberg Graduate School, Weizmann Institute of Science, Israel.

Korkhin, Y., Kalb, A. J., Peretz, M., Bogin, O., Burstein, Y. & Frolow, F. (1998). *J. Mol. Biol.* **278**, 967–981.

Korkhin, Y., Kalb, A. J., Peretz, M., Bogin, O., Burstein, Y. & Frolow, F. (1999). *Protein Sci.* **8**, 1241–1249.

Matthews, B. W. (1974). *J. Mol. Biol.* **82**, 513–526.

Otwinowski, Z. & Minor, W. (1997). *Methods Enzymol.* **276**, 307–326.

Peretz, M., Bogin, O., Tel-Or, S., Cohen, A., Li, G., Chen, J.-S. & Burstein, Y. (1997). *Anaerobe*, **3**, 259–270.

Samuelson, J., Zhang, W. W., Kumar, A., Descoteaux, S., Shen, P. S. & Bailey, G. (1992). *Arch. Med. Res.* **23**, 31–33.